IEEE Access
Multidisciplinary | Rapid Review | Open Access Journal

Received June 21, 2021, accepted July 6, 2021, date of publication July 8, 2021, date of current version July 16, 2021.

Digital Object Identifier 10.1109/ACCESS.2021.3095536

Modeling and Control of a Quadrotor UAV Equipped With a Flexible Arm in Vertical Plane

TIEHUA WANG[1], KAZUKI UMEMOTO[2], (Member, IEEE), TAKAHIRO ENDO[1], (Member, IEEE), AND FUMITOSHI MATSUNO[1], (Senior Member, IEEE)

[1]Department of Mechanical Engineering and Science, Kyoto University, Kyoto 615-8540, Japan
[2]Department of Mechanical Engineering, Nagaoka University of Technology, Niigata 940-2188, Japan

Corresponding author: Tiehua Wang (wantetuka@gmail.com)

ABSTRACT In the field of unmanned aerial vehicles (UAVs), aerial manipulations are receiving considerable attention because of their potential application to tasks such as pick and place, detection, and inspection. However, short flight endurance times and concerns about the safety to surroundings during interacting heavily limit the expansion of aerial manipulations in real implementations. To overcome these challenges, this paper focuses on a system in which a quadrotor UAV is equipped with a lightweight and flexible arm. Based on the infinite-dimensional dynamics, the mathematic model of system is described by a hybrid partial differential equation-ordinary differential equation (PDE-ODE). An easily implementable controller is derived from a Lyapunov functional construction related to the energy of the system. The proposed controller ensures global Lyapunov stability for nonlinear system and local asymptotic stability for the linearized system. Further, it is shown that the proposed controller realizes stable motion of the aerial manipulator as well as vibration control of the flexible arm. Finally, numerical simulations are conducted to investigate the validity of the proposed controller.

INDEX TERMS Unmanned aerial vehicle, aerial manipulation system, flexible arm, infinite-dimensional system, tip-position control, vibration suppression.

I. INTRODUCTION

By virtue of their high degree of mobility, unmanned aerial vehicles (UAVs) have been receiving considerable attention from both research communities and industries worldwide in the past decade. In particular, quadrotors have drawn more attention because of their various advantages such as simple structure, small size, and abilities including hovering and vertical take-off and landing, enabling them to perform many tasks such as surveying roads, monitoring wild animals, detecting small targets, and installing photovoltaic modules [1]–[3].

These successful applications of quadrotor UAVs are visual tasks that include aerial photography, remote sensing, and so on. Quadrotor UVAs are expected to also perform operating tasks such as pick and place, contact inspection, and manipulation, to truly extend their capacity in real environments [4]–[6]. Thus, quadrotor UAVs are intended to be equipped with robotic arms and to function as robotic workers and co-workers with manipulation skills [7].

In [8], [9], inspired by the high-speed hunting skills of birds of prey, grippers attached to a quadrotor to capture an object enabled the extension of a UAV's abilities from surveillance to carrying a payload. A nonredundant quadrotor manipulation system, in which a two degrees-of-freedom (DOF) robotic arm is attached to the bottom center of a quadrotor, is designed to perform pick-and-place missions in [10]. Redundant multi-DOF systems have been experimentally verified by indoor motion tracking and outdoor grasping operations, and have been applied to pick-and-place, insertion, and valve turning tasks in [11]–[14]. On the other hand, through physical interaction with the objective environment, aerial manipulators are available for industrial applications such as inspecting bridges and painting [15], [16]. Related to physical interaction by UAVs, we proposed a position/force hybrid controller for quadrotor UAVs with a multi-DOF manipulator in [17]. However, all those aerial manipulation systems are constituted by rigid and heavy arms, which incur crucial limitations.

One of the unavoidable issues is flight endurance time, which is the primary limitation for practical scenarios of aerial manipulation systems in potential industries.

The associate editor coordinating the review of this manuscript and approving it for publication was Yang Tang.

The weight of the arm further consumes battery power. Another obvious issue is safety. A rigid arm can hurt the surrounding environment or people when physically interacting with them.

To overcome the challenge of short flight endurance time, weight reduction is considered for the aerial manipulation system. In [18]–[20], several aerial manipulation systems with kinds of lightweight arms have been designed, but those arms are theoretically considered as rigid arm. In [21]–[25], aerial manipulation systems equip with compliant mechanisms on lightweight arms at joints or at the end effector, which the property of compliance might be friendly with the surroundings. However, all above-mentioned aerial manipulation systems do not take into account the deformation of lightweight links as well as the dynamics of flexibility in modeling and control.

Besides, a long-reach aerial manipulator consisting of a UAV body, a long and flexible link, and a short and rigid link connected with an end effector is proposed for inspection tasks considering flexibility [26]. However, the dynamic model is built on the basis of a finite-dimensional approximated model, and the internal stability of a system with a flexible link has not been demonstrated. It is known that the drawback of finite-dimensional approximation for a system with flexibility might result in spillover instability [27]. Therefore, it is important to control both the vibration of a flexible arm and the position of the end effector based on the infinite-dimensional dynamics of an aerial manipulation system.

In the field of tip-position control and vibration suppression for a flexible arm considering as an infinite-dimensional system, there have been several studies based on PDE-OED dynamics model. In [28], an exponential stabilization controller is proposed for the flexible beam to suppress the vibration, but the velocity of beam vibration assumed known or measurable which is rarely achieved during implementations. By applying piezoelectric actuators and sensors, the vibration of flexible beams can be asymptotically stabilized in [29]. Moreover, without using external assistant devices such as piezoelectric actuators, and unnecessary to assume unknown variables, the boundary controller has been investigated for stabilizing infinite-dimensional systems [30]–[32]. On the other hand, the strict stability of controller design is shown for kinds of flexible structures [33]–[36]. However, to the best of our knowledge, research on aerial manipulation system equipped with a flexible arm by applying a controller based on an infinite-dimensional model has not been reported.

To overcome these difficulties, in consideration of flight endurance times and safety to surroundings, we focuses on the aerial manipulation system that a quadrotor UAV equipped with a lightweight and flexible arm, and address on the modeling and control strategy of the system on the basis of infinite-dimensional dynamics. In contrast to finite-dimensional approximation for a system with flexibility, there is no issue of spillover instability when considering system based on the infinite-dimensional dynamics. In this paper, a controller of the aerial manipulation system is proposed for tracking the position of the end effector and suppressing the vibration of the flexible beam at the same time. The proposed controller does not need any hardly measurable information of flexible beam during implementations. It is worth mentioning that the control strategy of an aerial manipulation system considering infinite-dimensional dynamics has not been reported yet.

The originality of this paper includes the following:

(1) Derivation of a model consisting of partial differential equations (PDEs) and ordinary differential equations (ODEs), in consideration of infinite-dimensional dynamics for an aerial manipulator comprised of a quadrotor UAV and a flexible arm.

(2) Proposition of an easily implementable controller that stabilizes system Lyapunov stability globally and asymptotic stability locally.

(3) Presentation of the stability of the closed-loop system and execution of the proposed controller by numerical implementations.

This paper is organized as follows. The mathematical model of the controlled system and the control problem are described in Sec. II. The proposed controller and Lyapunov stability are then shown in Sec. III. The closed-loop system at the neighbourhood of the desired state and asymptotic stability are addressed in Sec. IV. Finally, numerical simulations and our conclusions are presented in Sec. V and Sec. VI, respectively.

II. CONTROLLED SYSTEM

A. DESCRIPTION

Fig. 1 shows an aerial manipulation system consisting of a one-link flexible arm and a rigid quadrotor UAV. One end of the arm is clamped to the rotational motor, and the other end has a tip mass. The quadrotor has a general symmetric structure, where a rotational motor for the flexible arm is mounted on the center of the body of the UAV. In this work, we consider that the quadrotor moves in the vertical plane and that the lightweight arm satisfies the Euler-Bernoulli beam hypothesis, for which we can ignore rotary-inertia and shear-deformation effects. In Fig. 2, Inertial Frame (IF) denotes the inertial reference coordinate and Body Frame (BF) is attached to the center of the symmetrical quadrotor. In addition, an Arm Frame (AF) is located at the revolute joint of the flexible arm connected to the quadrotor UAV. $\alpha(t)$ denotes the rotational angle of the arm motor in BF, and $\theta(t)$ is the orientational angle of the quadrotor UAV in IF. $w(r, t)$ is the transverse displacement of the flexible arm at time t and at spatial point $r(0 \leq r \leq L)$ in AF. The physical parameters used in this paper are summarized in Table 1.

We assume that the transverse displacement of the flexible arm and the orientational angle of the quadrotor UAV are small, i.e., the high-order nonlinear items of $w(r, t)$ can be ignored and $\sin\theta = \theta$, $\cos\theta = 1$.

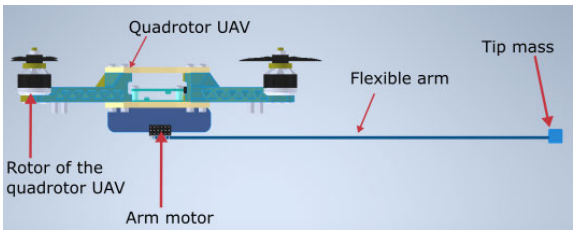

FIGURE 1. Structure diagram of quadrotor UAV equipped with a flexible arm.

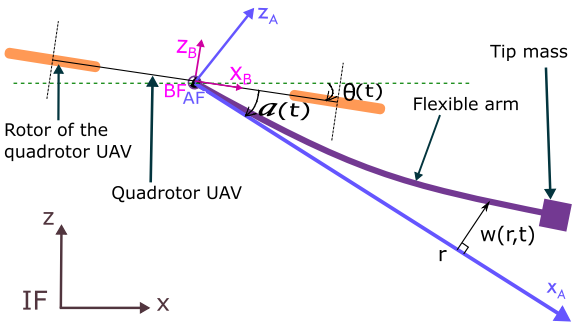

FIGURE 2. Schematic diagram of quadrotor UAV equipped with a flexible arm.

TABLE 1. Physical parameters.

Symbol	Description
J_b	moment of inertia of the quadrotor UAV
m_b	mass of the quadrotor UAV including the motor
J_m	moment of inertia of the motor rotor
L	length of the lightweight arm
ρ	uniform mass density per unit length of arm
m_a	mass of flexible arm $(=\rho\times L)$
EI	uniform flexible rigidity of arm
m_e	mass of arm tip

B. EQUATIONS OF MOTION

As the root of the flexible link is clamped to the vertical shaft of the rotor of the arm motor, the geometric boundary conditions are

$$w(0,t)=0,\quad w'(0,t)=0, \tag{1}$$

where the prime denotes the derivative with respect to the spatial variable r. Let $\zeta(t)$ and $p_r(r,t)$ be the position of the center of the quadrotor UAV and the flexible arm at a general point r in IF, respectively. $\zeta(t)$ and $p_r(r,t)$ are defined as follows:

$$\zeta=\begin{bmatrix}x & z\end{bmatrix}^T,\quad p_r=\begin{bmatrix}p_{rx} & p_{rz}\end{bmatrix}^T, \tag{2}$$

$$p_{rx}=x+rC_\beta+wS_\beta,\quad p_{rz}=z-rS_\beta+wC_\beta, \tag{3}$$

where $C_*=\cos(*)$, $S_*=\sin(*)$, $\beta=\theta+\alpha$. In order to simplify the notation of equations, the time variable is omitted and w, w_0, and w_e denote $w(r,t)$, $w(0,t)$, and $w(L,t)$ respectively.

The total kinetic energy T is comprised of: translational kinetic energy of quadrotor body K_{Bt}, rotational kinetic energy of quadrotor body K_{Br}, rotational kinetic energy of arm rotor K_M, kinetic energy of flexible arm K_A, and kinetic energy of tip mass K_E, shown as follows:

$$T=K_{Bt}+K_{Br}+K_M+K_A+K_E, \tag{4}$$

$$K_{Bt}=\frac{1}{2}m_b\dot\zeta^T\dot\zeta,\quad K_{Br}=\frac{1}{2}J_b\dot\theta^2,\quad K_M=\frac{1}{2}J_m\dot\beta^2,$$

$$K_A=\frac{1}{2}\int_0^L\rho\dot p_r^T\dot p_r dr,\quad K_E=\frac{1}{2}m_e\dot p_e^T\dot p_e, \tag{5}$$

where a dot denotes the derivative with respect to time t and $p_e=[p_{ex}\ \ p_{ez}]^T$ means $p_r(L,t)$.

The potential energy U consists of two sources, the gravity contribution U_g and the elastic contribution U_w, which can be obtained in IF as follows:

$$\begin{aligned}U&=U_g+U_w,\\ U_g&=m_bgz+\int_0^L\rho gp_{rgz}dr+m_egp_{egz},\\ U_w&=\int_0^L\rho gp_{rwz}dr+m_egp_{ewz}+\frac{1}{2}\int_0^L EI(w'')^2dr,\end{aligned} \tag{6}$$

where $p_{rgz}=z-rS_\beta$, $p_{rwz}=wC_\beta$, $p_{egz}=z-LS_\beta$, $p_{ewz}=w_eC_\beta$.

Further, the virtual work δW of the system is given by

$$\delta W=S_\theta f_B\delta x+C_\theta f_B\delta z+\tau_B\delta\theta+\tau_m\delta\alpha, \tag{7}$$

where $f_B(>0)$ and τ_B are the force and the torque, respectively, produced by the quadrotor UAV in BF, and τ_m is the torque of the arm motor. Then, Hamilton's principle gives

$$\begin{aligned}&\int_{t_1}^{t_2}(\delta T-\delta U+\delta W)dt\\ &=\int_{t_1}^{t_2}\Bigg[\left\{-m_b\ddot x-\int_0^L\rho\ddot p_{rx}dr-m_e\ddot p_{ex}+S_\theta f_B\right\}\delta x\\ &\quad+\left\{-m_b\ddot z-\int_0^L\rho\ddot p_{rz}dr-m_e\ddot p_{ez}-m_0g+C_\theta f_B\right\}\delta z\\ &\quad+\Bigg\{-J_b\ddot\theta-J_m\ddot\beta+\int_0^L\rho\ddot p_{rx}\left(rS_\beta-wC_\beta\right)dr\\ &\qquad+\int_0^L\rho\ddot p_{rz}\left(rC_\beta+wS_\beta\right)dr+m_e\ddot p_{ex}\left(LS_\beta-w_eC_\beta\right)\\ &\qquad+m_e\ddot p_{ez}\left(LC_\beta+w_eS_\beta\right)-m_eg\left(-w_eS_\beta-LC_\beta\right)\\ &\qquad-\int_0^L\rho g\left(-S_\beta w-rC_\beta\right)dr+\tau_B\Bigg\}\delta\theta\\ &\quad+\Bigg\{-J_m\ddot\beta+\int_0^L\rho\ddot p_{rx}\left(rS_\beta-wC_\beta\right)dr\\ &\qquad+\int_0^L\rho\ddot p_{rz}\left(rC_\beta+wS_\beta\right)dr+m_e\ddot p_{ex}\left(LS_\beta-w_eC_\beta\right)\\ &\qquad+m_e\ddot p_{ez}\left(LC_\beta+w_eS_\beta\right)-m_eg\left(-w_eS_\beta-LC_\beta\right)\\ &\qquad-\int_0^L\rho g\left(-S_\beta w-rC_\beta\right)dr+\tau_m\Bigg\}\delta\alpha-EIw_e''\delta w_e'\\ &\quad+\left\{-m_e\ddot p_{ex}S_\beta-m_e\ddot p_{ez}C_\beta-\left(m_egC_\beta-EIw_e'''\right)\right\}\delta w_e\\ &\quad+\int_0^L\left\{-\rho\ddot p_{rx}S_\beta-\rho\ddot p_{rz}C_\beta-\rho gC_\beta-EIw''''\right\}\delta w dr\Bigg]dt\\ &=0,\end{aligned} \tag{8}$$

where δ is a variation of the corresponding term and t_1 and t_2 are time. Since Eq. (8) exists for the arbitrary variations δx, δz, $\delta\theta$, $\delta\alpha$, $\delta w'_e$, δw_e, and δw, under the assumption described in Sec. II-A that $\sin\theta = \theta$, $\cos\theta = 1$, a simple calculation of this variational principle leads to the following equations of motion:

$$\begin{cases} m_0\ddot{x} + f_x = \theta f_B, \\ m_0\ddot{z} + f_z + m_0 g = f_B, \\ J_b\ddot{\theta} = \tau_B - \tau_m, \\ J_m\ddot{\beta} + EIw''_0 - d_\tau = \tau_m, \\ w(0,t) = 0, \quad w'(0,t) = 0, \quad w''_e = 0, \\ EI(\dfrac{m_e}{\rho}w''''_e + w''''_e) = 0, \\ \ddot{w} + \ddot{x}S_\beta + \ddot{z}C_\beta - r\ddot{\beta} + gC_\beta + \dfrac{EI}{\rho}w'''' = 0, \end{cases} \tag{9}$$

where $m_0 = m_b + m_a + m_e$, and f_x, f_z, d_τ are the coupling nonlinear dynamic items relative to the rigid quadrotor UAV and flexible arm shown as follows,

$$\begin{aligned} f_x = &\int_0^L \rho\left(-rC_\beta\dot{\beta}^2 - rS_\beta\ddot{\beta} - wS_\beta\dot{\beta}^2 + wC_\beta\ddot{\beta} + 2C_\beta\dot{\beta}\dot{w}\right. \\ &\left. + S_\beta\ddot{w}\right)dr - m_eLC_\beta\dot{\beta}^2 - m_eLS_\beta\ddot{\beta} - w_em_eS_\beta\dot{\beta}^2 \\ &+ w_em_eC_\beta\ddot{\beta} + 2m_eC_\beta\dot{\beta}\dot{w}_e + m_eS_\beta\ddot{w}_e, \\ f_z = &\int_0^L \rho\left(rS_\beta\dot{\beta}^2 - rC_\beta\ddot{\beta} - wC_\beta\dot{\beta}^2 - wS_\beta\ddot{\beta} - 2S_\beta\dot{\beta}\dot{w}\right. \\ &\left. + C_\beta\ddot{w}\right)dr + m_eLS_\beta\dot{\beta}^2 - m_eLC_\beta\ddot{\beta} - w_em_eC_\beta\dot{\beta}^2 \\ &- w_em_eS_\beta\ddot{\beta} - 2m_eS_\beta\dot{\beta}\dot{w}_e + m_eC_\beta\ddot{w}_e, \\ d_\tau = &\int_0^L w\rho\left(-\ddot{x}C_\beta + \ddot{z}S_\beta + r\dot{\beta}^2 - 2\dot{\beta}\dot{w} + gS_\beta\right)dr \\ &+ m_ew_e(-\ddot{x}C_\beta + \ddot{z}S_\beta + L\dot{\beta}^2 - 2\dot{\beta}\dot{w} + gS_\beta). \end{aligned} \tag{10}$$

Here, f_x, f_z, and d_τ are coupling nonlinear dynamic terms between the quadrotor UAV and the flexible arm, whose values are rarely known because of the difficulty of obtaining the value of transverse displacement w and its time derivatives. f_x and f_z can be canceled by the controller proposed in formulation of the derivative of V in the proof of Theorem 1, whereas d_τ cannot be canceled. We consider d_τ as the disturbance of system and estimate d_τ by using a disturbance observer, which will be further explained in next section.

C. CONTROL OBJECTIVE

The aims of this paper are to control the position of the end effector of an aerial manipulator and to suppress the vibration of the flexible arm at the same time. Obviously, the motion of the end effector can be achieved when both the quadrotor UAV hovers at a desired position ζ_d and the rotational angle of the arm motor converges to the desired value α_d simultaneously. Therefore, under this equilibrium, the state of the aerial manipulation system holds

$$x = x_d,\ z = z_d,\ \beta = \beta_d,\ \theta = 0,\ \dot{x} = \dot{z} = \dot{\beta} = 0,\ \dot{w} = 0. \tag{11}$$

On the other hand, the flexible arm would have a deformation $w_\epsilon(r)$ at the equilibrium because of gravity. Substituting states (11) into system (9), we have

$$w_\epsilon = \frac{gC_{\beta_d}}{EI}\left(\frac{1}{6}(m_a+m_e)r^3 - \frac{1}{2}(\frac{1}{2}m_a + m_e)Lr^2 - \frac{1}{24}\rho r^4\right). \tag{12}$$

On the basis of these results, the control objective is to design a controller satisfying

$$\begin{cases} e_x \to 0,\ e_z \to 0,\ e_\beta \to 0, \\ \dot{x} \to 0,\ \dot{z} \to 0,\ \dot{\beta} \to 0,\ \dot{\theta} \to 0, \quad \text{as } t \to \infty \\ w(r,t) \to w_\epsilon(r),\ \dot{w}(r,t) \to 0, \end{cases} \tag{13}$$

where $e_x = x - x_d, e_z = z - z_d,\ e_\beta = \beta - \beta_d$.

III. PROPOSED CONTROLLER

In this section, we propose a controller to stabilize the aerial manipulation system Lyapunov stability globally and asymptotic stability at the neighborhood of the desired state. This control objective would be achieved by controlling the position of the end effector and suppressing the vibration of the flexible arm.

In our control strategy, we design the input of arm motor τ_m to control the angle and suppress the vibration of the flexible arm. At the same time, we design the inputs of the quadrotor UAV f_B and τ_B to control the position of the aerial base. That is to say, on the level of torque, the inputs of torques τ_m and τ_B respectively control the flexible arm and the quadrotor UAV. On the other hand, on the level of force, the input of force f_B is in control of the whole aerial manipulation system.

Between the quadrotor UAV and the flexible arm, there are coupling nonlinear dynamics terms, f_x, f_z, and d_τ, as shown in Eq. (10), whose values are rarely known because of the difficulty of obtaining the value of transverse displacement w and its time derivatives. In an aerial manipulation system, the performance of coupling dynamics would be expressed as force and torque, and can be viewed as the interaction between the quadrotor UAV and the flexible arm, where f_x, f_z show the coupling dynamics on the level of force while d_τ has same unit with the torque. Since the inputs of torques are designed individually, we need to investigate and estimate the coupling dynamics item d_τ. Note that the estimation of coupling dynamics terms f_x, f_z is unnecessary because the quadrotor UAV and the flexible arm are considered simultaneously.

Here, we consider d_τ as a disturbance in dynamics and use a disturbance observer to estimate d_τ. Thus, the control input τ_m can be designed as

$$\tau_m = \tau_{m0} + \tau_{m1}, \tag{14}$$

where τ_{m1} denotes a disturbance observer feedback input for the disturbance attenuation corresponding to an inner loop, while τ_{m0} is an input for stabilizing a disturbance-eliminated system corresponding to an outer loop. According to the

dynamics equation for a flexible arm in Eq. (9), we have

$$d_\tau = J_m\ddot{\beta} + EIw_0'' - \tau_{m0} - \tau_{m1}, \tag{15}$$

and the disturbance observer [37] is designed as

$$\dot{\hat{d}}_\tau = -\hat{d}_\tau/T + (J_m\ddot{\beta} + EIw_0'' - \tau_{m0} - \tau_{m1})/T, \tag{16}$$

using a first-order low-pass filter of (15), where T is a positive constant. Although Eq. (16) includes state derivative $\ddot{\beta}$, it can be transformed to the align $\dot{\beta}/T$ without the state derivative. The disturbance observer feedback input τ_{m1} is designed as

$$\tau_{m1} = -\frac{k_7}{1+k_7}\hat{d}_\tau. \tag{17}$$

We suppose that the inner loop runs much faster than the outer loop, the disturbance of which can be estimated well enough and can be eliminated by (16), which means we have

$$\hat{d}_\tau = d_\tau. \tag{18}$$

Note that Eq. (18) only can be obtained under the assumption that Eq. (16) quickly converges by selecting enough small T.

Theorem 1: For the aerial manipulation system (9) with (17), if the control inputs are designed as

$$\begin{cases} \tau_m = \tau_{m0} + \tau_{m1}, \\ \tau_{m0} = \dfrac{1}{1+k_7}\left(k_7EIw_0'' - k_8e_\beta - k_9\dot{\beta} - G\right), \\ \tau_B = \tau_m + J_b(\dot{\phi}_1 - k_4\eta_1 - \eta_0), \\ f_B = (m_0g - k_5e_z - k_6\dot{z}), \end{cases} \tag{19}$$

then the system can be Lyapunov stable globally, where G, ϕ_0, η_0, ϕ_1 and η_1 are shown as follows,

$$G = (\frac{1}{2}m_a + m_e)gLC_\beta, \tag{20}$$

$$\phi_0 = -\frac{k_1}{f_B}e_x - \frac{k_2}{f_B}\dot{x}, \tag{21}$$

$$\eta_0 = \theta - \phi_0, \tag{22}$$

$$\phi_1 = \dot{\phi}_0 - k_3\eta_0 - f_B\dot{x}, \tag{23}$$

$$\eta_1 = \dot{\theta} - \phi_1, \tag{24}$$

and $k_i > 0 (i = 1, 2, \cdots, 9)$.

Proof: Let us consider the candidate Lyapunov function

$$V = V_1 + V_2, \tag{25}$$

where V_1 is the energy part of the system while V_2 is the state variable part, shown as follows:

$$V_1 = K_{Bt} + K_M + K_A + K_E + U_w, \tag{26}$$

$$V_2 = \frac{k_1}{2}e_x^2 + \frac{k_5}{2}e_z^2 + \frac{k_7}{2}J_m\dot{\beta}^2 + \frac{k_8}{2}e_\beta^2 + \frac{1}{2}\eta_0^2 + \frac{1}{2}\eta_1^2. \tag{27}$$

By differentiating Eq. (26) with respect to time, the following identity is obtained:

$$\dot{V}_1 = \dot{x}\theta f_B + \dot{z}(f_B - m_0g) + \dot{\beta}\left(\tau_m + G\right), \tag{28}$$

where the derivation can be found in Appendix A.

On the other hand, from Eqns. (22),(23), and (24), we have

$$\dot{\eta}_0 = \eta_1 - k_3\eta_0 - f_B\dot{x}. \tag{29}$$

From Eq. (24), and employing the equation of motion in Eq. (9), we obtain

$$\dot{\eta}_1 = \ddot{\theta} - \dot{\phi}_1 = \frac{1}{J_b}(\tau_B - \tau_m) - \dot{\phi}_1. \tag{30}$$

By differentiating Eq. (27) with respect to time, and by substituting (22), (29), and (30), we have

$$\begin{aligned} \dot{V}_2 = {} & k_1\dot{x}e_x + k_5\dot{z}e_z + k_7\dot{\beta}(\tau_m - EIw_0'' + d_\tau) \\ & + k_8\dot{\beta}e_\beta + \eta_0(\eta_1 - k_3\eta_0) - (\theta - \phi_0)f_B\dot{x} \\ & + \eta_1\left(\frac{1}{J_b}(\tau_B - \tau_m) - \dot{\phi}_1\right). \end{aligned} \tag{31}$$

Combining (28) and (31), and substituting control inputs Eq. (19) with (17), we get

$$\begin{aligned} \dot{V} &= \dot{V}_1 + \dot{V}_2 \\ &= \dot{\beta}\left\{(1+k_7)\tau_m - k_7EIw_0'' + k_7d_\tau + k_8e_\beta + G\right\} \\ &\quad + \dot{z}(f_B - m_0g + k_5e_z) + \dot{x}(\phi_0f_B + k_1e_x) \\ &\quad + \eta_0(\eta_1 - k_3\eta_0) + \eta_1\left(\frac{1}{J_b}(\tau_B - \tau_m) - \dot{\phi}_1\right) \\ &= \dot{\beta}\left\{(1+k_7)\tau_{m1} + k_7d_\tau\right\} \\ &\quad + \dot{\beta}\left\{(1+k_7)\tau_{m0} - k_7EIw_0'' + k_8e_\beta + G\right\} \\ &\quad + \dot{z}(f_B - m_0g + k_5e_z) + \dot{x}(-k_2\dot{x}) - k_3\eta_0^2 - k_4\eta_1^2 \\ &= -k_9\dot{\beta}^2 - k_6\dot{z}^2 - k_2\dot{x}^2 - k_3\eta_0^2 - k_4\eta_1^2 \\ &\le 0. \end{aligned}$$

Now, from the Lyapunov method, we know that the system becomes Lyapunov stable. ■

Note that Theorem 1 only indicates the global Lyapunov stability of the closed-loop system and cannot ensure the control objective in Section II-C. In next section, we will show the local asymptotic stability of the linearized closed-loop system with the proposed controller to confirm achievement of the control objective in Section II-C.

For the control input τ_{m0} in Eq. (19), designed for the flexible arm, the second and third terms are the proportional-derivative (PD) control of the angle, and the first term is the feedback of the strain (S) at the root of the flexible arm. Thus, the controller of the flexible arm is called PDS control. The fourth term is the gravity compensation term. In the proposed controller (19), the states of the quadrotor UAV can be obtained from sensors and filters, α is the other component of $\beta(\beta = \alpha + \theta)$ besides the quadrotor's attitude θ and is measured by the encoder, $\dot{\beta}$ is obtained by the numerical difference method, and w_0'' is measured by the strain gauges. Therefore, the proposed design with PDS control is easily implemented.

IV. STABILITY AT THE NEIGHBORED OF THE DESIRED STATE

In this section, we prove that the proposed controller (19) with (17) can ensure the asymptotic stability of the

closed-loop system at the neighborhood of the desired state. The sketch of the proof is as follows: first we show that LaSalle's invariance principle can be applied to this infinite-dimensional aerial manipulation system, then we derive the solution of the system that satisfies the conditions for the invariant set, and finally we use this solution to show that the invariant set has only the desired state. Besides, in order to apply LaSalle's invariance principle to infinite-dimensional systems, the closed-loop system must be formulated in a functional space such as a Hilbert space.

A. LINEARIZED EQUATIONS OF MOTION IN A HILBER SPACE

In the neighborhood of the desired state, the quadrotor UAV hovers at the equilibrium point and the flexible arm hangs around the assigned angle. If we let $x(t) = x_d + \Delta x(t), z(t) = z_d + \Delta z(t), \beta(t) = \beta_d + \Delta\beta(t), \Delta\beta(t) = \Delta\alpha(t) + \theta(t), w(r,t) = w_\epsilon(r) + \Delta w(r,t)$, then variables $\Delta x(t), \Delta z(t), \theta(t), \Delta w(t), \Delta\beta(t), \Delta\dot{x}(t), \Delta\dot{z}(t)$ and $\Delta\dot{\beta}(t)$ would be small. Besides, from the equations as shown in Eq. (9): $w(0,t) = 0, w'(0,t) = 0, w''_e = 0$, and Eq. (12), we can know that

$$\Delta w(0,t) = 0, \quad \Delta w'(0,t) = 0, \quad \Delta w''(L,t) = 0. \tag{32}$$

Let us introduce the following new variable,

$$\Delta w_\beta(r,t) = S_{\beta_d}\Delta x(t) + C_{\beta_d}\Delta z(t) - r\Delta\beta(t) + \Delta w(r,t), \tag{33}$$

by substituting Eqns. (17) and (19) into Eq. (9), then the closed-loop system can be linearized as follows:

$$\begin{cases} \Delta\ddot{x} = -\dfrac{k_1}{m_0}\Delta x - \dfrac{k_2}{m_0}\Delta\dot{x}, \\ \Delta\ddot{z} = -\dfrac{k_5}{m_0}\Delta z - \dfrac{k_6}{m_0}\Delta\dot{z}, \\ \Delta\ddot{\beta} = \dfrac{-k_8\Delta\beta - k_9\Delta\dot{\beta} - EI\,\Delta w''_\beta(0)}{J_m(1+k_7)}, \\ \ddot{\theta} = -(k_3k_4+1)\theta - (k_3+k_4)\dot{\theta}, \\ \Delta\ddot{w}_\beta(L) = \dfrac{EI}{m_e}\Delta w'''_\beta(L), \\ \Delta\ddot{w}_\beta = -\dfrac{EI}{\rho}\Delta w''''_\beta, \end{cases} \tag{34}$$

and the boundary conditions are shown as

$$\begin{aligned} &\Delta w_\beta(0) = S_{\beta_d}\Delta x + C_{\beta_d}\Delta z, \\ &\Delta w'_\beta(0) = -\Delta\beta, \quad \Delta w''_\beta(L) = 0, \end{aligned} \tag{35}$$

where the time variable is omitted and $\Delta w_\beta(0)$, $\Delta w'_\beta(0)$, and $\Delta w''_\beta(L)$ denote $\Delta w_\beta(0,t)$, $\Delta w'_\beta(0,t)$, and $\Delta w''_\beta(L,t)$ respectively. On the other hand, the following functional space H is introduced as the state space:

$$\begin{aligned} H = \Big\{ & y : u_w \in H^2(0,L), v_w \in L^2(0,L), v_e \in R, \\ & u'_w(0) = -u_3, u_w(0) = S_{\beta_d}u_1 + C_{\beta_d}u_2, \\ & u_i \in R, v_i \in R, \quad i = 1,\cdots,4 \Big\}, \end{aligned} \tag{36}$$

where $y = [u_1, v_1, u_2, v_2, u_3, v_3, u_4, v_4, v_e, u_w, v_w]^T$, H^2 denotes a second-order Sobolev space, and L^2 is the square integrable space. In H we define the following inner product:

$$\begin{aligned} \langle y, \hat{y}\rangle_H = & \frac{1}{2}m_0(v_1\hat{v}_1 + v_2\hat{v}_2) + \frac{1+k_7}{2}J_m v_3\hat{v}_3 + \frac{1}{2}v_4\hat{v}_4 \\ & + \frac{1}{2}\int_0^L \rho v_w\hat{v}_w dr + \frac{1}{2}\int_0^L EIu''_w\hat{u}''_w dr + \frac{1}{2}m_e v_e\hat{v}_e \\ & + \frac{k_1}{2}u_1\hat{u}_1 + \frac{k_5}{2}u_2\hat{u}_2 + \frac{k_8}{2}u_3\hat{u}_3 + \frac{k_3k_4+1}{2}u_4\hat{u}_4, \end{aligned} \tag{37}$$

where

$$y = \begin{bmatrix} u_1 & v_1 & \cdots & u_4 & v_4 & v_e & u_w & v_w \end{bmatrix}^T, \tag{38}$$

$$\hat{y} = \begin{bmatrix} \hat{u}_1 & \hat{v}_1 & \cdots & \hat{u}_4 & \hat{v}_4 & \hat{v}_e & \hat{u}_w & \hat{v}_w \end{bmatrix}^T. \tag{39}$$

Lemma 1: The space H together with the inner product given by (37) becomes a Hilbert space.

Proof: See Appendix B ■

Then we define the unbounded linear operator $A : D(A) \subset H \to H$ as follows:

$$Ay = \begin{bmatrix} v_1 \\ -\dfrac{k_1}{m_0}u_1 - \dfrac{k_2}{m_0}v_1 \\ v_2 \\ -\dfrac{k_5}{m_0}u_2 - \dfrac{k_6}{m_0}v_2 \\ v_3 \\ \dfrac{1}{J_m(1+k_7)}\left(-k_8u_3 - k_9\,v_3 - EIu''_w(0)\right) \\ v_4 \\ -(k_3k_4+1)u_4 - (k_3+k_4)v_4 \\ \dfrac{EI}{m_e}u'''_w(L) \\ v_w \\ -\dfrac{EI}{\rho}u''''_w \end{bmatrix}, \tag{40}$$

where the domain of the operator A is defined as

$$\begin{aligned} D(A) = \Big\{ & y \in H : u_w \in H^4(0,L), v_w \in H^2(0,L), \\ & u_w(0) = S_{\beta_d}u_1 + C_{\beta_d}u_2, u'_w(0) = -u_3, \\ & u''_w(L) = 0, v_w(0) = 0, v'_w(0) = -v_3, \\ & v_w(L) = v_e, u_i \in R, v_i \in R, i = 1,\cdots,4 \Big\}. \end{aligned} \tag{41}$$

Then the closed-loop system under the Hilbert space H can be written as the first-order evolution equation

$$\dot{y} = Ay, \tag{42}$$

where

$$y = [\Delta x, \Delta\dot{x}, \Delta z, \Delta\dot{z}, \Delta\beta, \Delta\dot{\beta}, \theta, \dot{\theta}, \Delta\dot{w}_\beta(L), \Delta w_\beta, \Delta\dot{w}_\beta]^T.$$

B. APPLICATION OF LaSalle's INVARIANCE PRINCIPLE

To apply LaSalle's invariance principle, we need to investigate whether the properties of the closed-loop system (42) satisfy the following lemma:

Lemma 2: The operator A generates a C_0-semigroup of contractions. Furthermore, the operator A^{-1} is compact.

Proof: To prove that the operator A generates a C_0-semigroup of contractions, from the Lumer-Phillips theorem [38], we need to show that 1) operator A is dissipative and 2) $0 \in \rho_A(A)$, where $\rho_A(A)$ is the resolvent set of the operator A. First, we show that the operator A is dissipative. For any given $y = [u_1, v_1, u_2, v_2, u_3, v_3, u_4, v_4, v_e, u_w, v_w]^T \in D(A)$, the result of inner product satisfies

$$\langle Ay, y\rangle_H = -\frac{k_2}{2}v_1^2 - \frac{k_6}{2}v_2^2 - \frac{k_9}{2}v_3^2 - \frac{k_3}{2}u_4^2 - \frac{k_3+k_4}{2}v_4^2 \le 0, \tag{43}$$

where the derivation details can be found in Appendix C. Thus, the operator A is dissipative.

Next, we show that $0 \in \rho_A(A)$. In order to prove $0 \in \rho_A(A)$, we can show that the operator A^{-1} exists and is bounded. That is to say, for any given $\psi = [l_1, h_1, l_2, h_2, l_3, h_3, l_4, h_4, h_e, l_w, h_w]^T \in H$, we have to find $\phi = [u_1, v_1, u_2, v_2, u_3, v_3, u_4, v_4, v_e, u_w, v_w]^T \in D(A)$ that satisfies $A\phi = \psi$. By directly solving $A\phi = \psi$, we obtain

$$\begin{cases} u_1 = -\dfrac{m_0}{k1}(h_1 + \dfrac{k_2}{m_0}l_1), \\ v_1 = l_1, \\ u_2 = -\dfrac{m_0}{k_5}(h_2 + \dfrac{k_6}{m_0}l_2), \\ v_2 = l_2, \\ u_3 = -\left(J_m(1+k_7)h_3 + k_9\, l_3 + EIu_w''(0)\right)/k_8, \\ v_3 = l_3, \\ u_4 = -\dfrac{1}{k_3k_4+1}(h_4 + (k_3+k_4)l_4), \\ v_4 = l_4, \\ v_e = v_w(L) = l_w(L), \\ u_w = c_{w0} + c_{w1}r + \dfrac{c_{w2}}{2}r^2 + \dfrac{c_{w3}}{6}r^3 \\ \quad + \dfrac{\rho}{EI}\displaystyle\int_0^r\int_0^{r_1}\int_0^{r_2}\int_0^{r_3} h_w(r_4)dr_4\, dr_3 dr_2 dr_1, \\ v_w = l_w(r), \end{cases} \tag{44}$$

where $c_{w_j}(j = 0, 1, 2, 3)$ are constants determined by the boundary conditions, including $c_{w3} + \frac{\rho}{EI}\int_0^L h_w(r)dr = -\frac{m_e}{EI}h_e$. Then we find that the operator A^{-1} exists, and $\phi = A^{-1}\psi$. It is can be shown that there exists a positive constant K that satisfies

$$\| \phi \|_H = \| A^{-1}\psi \|_H \le K \| \psi \|_H, \tag{45}$$

where the derivation can be found in Appendix D. Therefore, the operator A^{-1} is bounded, and thus $0 \in \rho_A(A)$ is obtained. Finally, the following estimation can be obtained using the same procedure we used for the derivation of Eq. (45):

$$\| \phi \|_{H_2} \le K' \| \psi \|_H,$$

where $H_2 = H^4(0, L) \times H^2(0, L) \times R^9$, $\| \cdot \|_{H_m}$ is the usual norm in the Sobolev space H_m, and K' is a positive constant. This means the operator A^{-1} maps the bounded sets of H into the bounded sets of H_2. According to the Sobolev embedding theorem [39], the embedding of H_2 in H is compact, and thus the operator A^{-1} is compact. ■

C. ASYMPTOTIC STABILITY

From LaSalle's invariance principle [40], all solutions of Eq. (42) asymptotically converge to the maximal invariant subset of the following set

$$\Omega = \left\{ y \in H \mid \dot{W} = 0 \right\}, \tag{46}$$

where $W = \langle y, y\rangle_H = \| y \|_H^2$ is the Lyapunov function. Here, it is shown that $\Omega \in H$ contains only the zero solution.

Lemma 3: For the invariant set Ω, we find that it contains only $\Delta x = 0,\ \Delta z = 0,\ \Delta\beta = 0,\ \theta = 0, \Delta w = 0,\ \Delta\dot{x} = 0,\ \Delta\dot{z} = 0,\ \Delta\dot{\beta} = 0,\ \dot{\theta} = 0, \Delta\dot{w} = 0.$

Proof: Under the conditions for the invariant set, $dW/dt = 0$ gives us

$$-k_2\Delta\dot{x}^2 - k_6\Delta\dot{z}^2 - k_9\Delta\dot{\beta}^2 - k_3\theta^2 - (k_3+k_4)\dot{\theta}^2 = 0, \tag{47}$$

which implies that

$$\Delta\dot{x} = 0,\ \Delta\dot{z} = 0,\ \Delta\dot{\beta} = 0,\ \theta = 0,\ \dot{\theta} = 0, \tag{48}$$

$$\Delta\ddot{x} = 0,\ \Delta\ddot{z} = 0,\ \Delta\ddot{\beta} = 0. \tag{49}$$

Substituting (48), (49) into Eq. (34) yields

$$\Delta x = 0,\ \Delta z = 0,\ \Delta\beta = 0, \tag{50}$$

$$\Delta w_0'' = c_0, \tag{51}$$

$$EI(\frac{m_e}{\rho}\Delta w_e'''' + \Delta w_e'''') = 0, \tag{52}$$

$$\Delta\ddot{w} + \frac{EI}{\rho}\Delta w'''' = 0, \tag{53}$$

where c_0 is a constant. From Eq. (53), we know that the solution would be

$$\Delta w(r, t) = \Delta w_1(t)\Delta w_2(r), \tag{54}$$

Substituting (54) into (53), we have

$$\frac{\Delta\ddot{w}_1}{\Delta w_1} = -\frac{EI}{\rho}\frac{\Delta w_2''''}{\Delta w_2}, \tag{55}$$

and then we know that (55) equals a constant. Suppose that $\frac{\Delta w_2''''}{\Delta w_2} = \lambda_w$, where λ_w is a constant, and thus we obtain

$$\Delta w_1(t) = c_1 \sin\left(\sqrt{\lambda_w\frac{EI}{\rho}}t + \psi_0\right), \tag{56}$$

$$\Delta w_2(r) = c_2 e^{-\sqrt[4]{\lambda_w}r} + c_4 e^{\sqrt[4]{\lambda_w}r} + c_3\sin(\sqrt[4]{\lambda_w}r) + c_5\cos(\sqrt[4]{\lambda_w}r), \tag{57}$$

where $c_i(i = 1, 2, \cdots, 5)$ and ψ_0 are constants. Now, we consider the following two cases: $\lambda_w = 0$ and $\lambda_w \neq 0$.

1) $\lambda_w = 0$

From Eq. (57), we know that $\Delta w_2(r) = \Delta w_2(0)$, and

from Eq. (54) and $\Delta w(0,t)=0$ as shown in Eq. (32), then we have

$$\Delta w(r,t)=\Delta w_1(t)\Delta w_2(0)=\Delta w(0,t)=0. \quad (58)$$

2) $\lambda_w \neq 0$
Now, we consider the following two cases: $c_1=0$ and $c_1\neq 0$.

- $c_1=0$:
From Eq. (56) we know that $\Delta w_1(t)=0$, and then we have

$$\Delta w(r,t)=\Delta w_1(t)\Delta w_2(r)=0. \quad (59)$$

- $c_1\neq 0$:
From Eq. (32), we obtain that

$$\Delta w_2(0)=0,\ \Delta w_2'(0)=0,\ \Delta w_2''(L)=0, \quad (60)$$

In addition, from Eqns. (51) and (52), we have

$$w_2''(0)=0,\ \frac{m_e}{\rho}\Delta w_2''''(L)+\Delta w_2'''(L)=0. \quad (61)$$

From (60) and (61), then we can derive that $c_i(i=2,3,\cdots,5)=0$, $\Delta w_2(r)=0$, and thus we have

$$\Delta w(r,t)=\Delta w_1(t)\Delta w_2(r)=0. \quad (62)$$

In summary, under all cases as shown in Eqns. (58), (59) and (62), we can obtain

$$\Delta w=0. \quad (63)$$

And further,

$$\Delta \dot{w}=0. \quad (64)$$

Therefore, we know Lemma 3 is proved. ■

Finally, the following theorem for the asymptotic stability of the closed-loop system is obtained:

Theorem 2: The closed-loop system (42) is asymptotically stable.

Proof: From Lemma 2, it is easy to see that $0\in$ range(A). Further, from Theorem 6.29 in [41] and the fact that the operator A^{-1} is compact, the operator $(\lambda I-A)^{-1}$ is compact for every $\lambda\in\rho_A(A)$. This implies the precompactness of the solution trajectory by Theorem 3.65 in [40]. Therefore, from Lemma 3 and LaSalle's invariant principle (Theorem 3.64 in [40]), the closed-loop system (42) is asymptotically stable. ■

Therefore, we have $\Delta x=\Delta z=\Delta\beta=\theta=\Delta w=0$ and $\Delta\dot{x}=\Delta\dot{z}=\Delta\dot{\beta}=\dot{\theta}=\Delta\dot{w}=0$ as $t\to\infty$ from Lemma 3. Further, the control objective (13) is achieved.

V. NUMERICAL SIMULATION

A. SIMULATION SETUP

To evaluate the performance of the proposed control strategy, we carried out numerical simulations. For these simulations, the finite-dimensional approximated model was derived by the Galerkin approximations considering the first seven vibration modes. More details can be found in reference [42].

The arm is considered a thin stainless steel plate 1m length, 0.002m thickness, and 0.04m width. From the physical constants and the geometric shape of the arm, we have

$$L=1\text{m},\quad \rho=0.45\text{kg/m},\quad m_a=0.45\text{kg},$$
$$E=2.06\times10^{11}\text{N/m}^2,\quad I=1.944\times10^{-11}\text{m}^4. \quad (65)$$

Plant parameters of the quadrotor UAV and arm motor are

$$m_b=1.2\text{kg},\quad J_b=0.004\text{kg}\cdot\text{m}^2,$$
$$m_e=0.2\text{kg},\quad J_m=0.0006\text{kg}\cdot\text{m}^2. \quad (66)$$

In this simulation, we investigate the response when both the quadrotor UAV and the flexible arm moving toward desired positions. The initial state was set as $x(0)=z(0)=\theta(0)=\beta(0)=0$ and $\dot{x}(0)=\dot{z}(0)=\dot{\theta}(0)=\dot{\beta}(0)=0$, while the desired state was $x_d=3$, $z_d=2$, $\beta_d=\pi/10$; thus, the static deformation would be $w_\epsilon(L)=-0.21$m according to Eq. (12). Besides, the feedback gains were set as $k_1=10$, $k_2=3$, $k_3=18$, $k_4=6, k_5=5$, $k_6=3$, $k_7=5.5$, $k_8=25, k_9=3.5$. The parameter tuning is performed by trial and error. We set the controller's sampling time $\Delta t=0.005$s, and the disturbance observer was set to run 50 times faster than the controller.

To the best of our knowledge, a controller for an aerial manipulation system considering infinite-dimensional dynamics has not been reported before. Therefore, there are few controllers for comparison. In order to investigate the validation of the proposed control strategy, we conducted a comparison of the controller for the flexible arm in the proposed design (19), which is the PDS controller

$$\tau_{m0}=\frac{1}{1+k_7}\left(k_7EIw_0''-k_8e_\beta-k_9\dot{\beta}-G\right) \quad (67)$$

comparing with the PD controller

$$\tau_{m0}=\frac{1}{1+k_7}\left(-k_8e_\beta-k_9\dot{\beta}-G\right). \quad (68)$$

B. SIMULATION 1

We implemante the simulation without disturbance or noise at first, and the comparison results are shown as Fig. 3-Fig. 6. In Fig. 3 and Fig. 4, the solid lines show the responses of the controller with PDS flexible arm control, while the stippled lines show the response of the controller with PD flexible arm control.

In Fig. 3, (a)(c)(e) on the left side are the states' responses of the quadrotor UAV while (g) shows the sum of the orientational angle of the quadorotor UAV and the rotational angle of the arm motor. In Fig. 3, (b)(d) are the needed force and torque of the quadrotor UAV, while (f) is the needed torque of the arm motor. These values are reasonable for real actuators. From (a)(c) in Fig. 3, error values of the positions of the quadrotor UAV converged to 0 because they were governed by the same controller, while the responses of angles shown in (e)(g) were different because of the coupling dynamics with the flexible arm where the controller was different. Specifically, the controller with PDS flexible arm control stabilized system

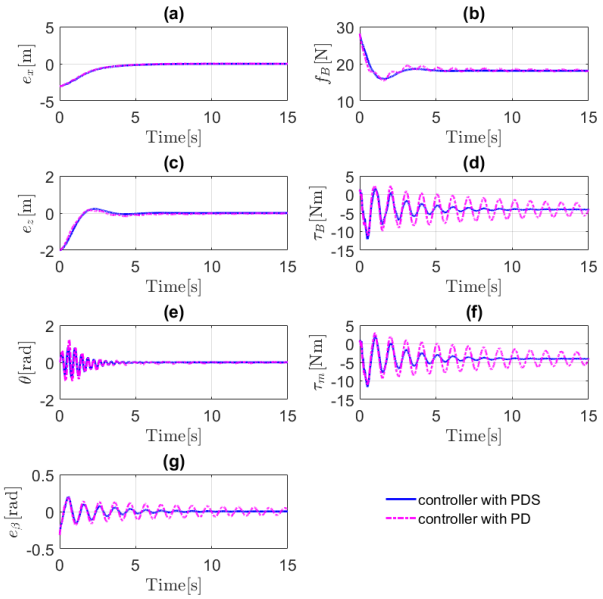

FIGURE 3. Comparison of responses of states and needed inputs.

in 10 seconds and the error of rotational angle becomed 0, while the error of rotational angle was larger than 0.07rad after 10 seconds for the controller with PD flexible arm control. In fact, the root mean squared error value of e_β in the response of the controller with PDS flexible arm control was $E_{e_\beta} = \|e_\beta\| = 0.0518$, while this value in the controller with PD flexible arm control was $E_{e_\beta} = \|e_\beta\| = 0.0776$, where $\|\cdot\| = \sqrt{\frac{1}{N}\Sigma_1^N(\cdot)^2}$ and N is the total number of samples.

Apparently, the PDS control of the flexible arm performed better, which is clearly shown in Fig. 4 and Fig. 5. Fig. 4 shows the time responses of the flexible arm, where $w(L,t)$ in 4(a) is the transverse displacement of the end effector at the flexible arm, (b) is the rotational angle velocity, (c) is the bending moment at the root of the arm, and (d) is the vibration velocity of the end effector. Fig. 5 shows the whole beam deformation along time and displacement, where (a) is under the controller with PDS while (b) is with PD. From Fig. 4 and Fig. 5, we find that the vibration was suppressed in 10 seconds by the proposed controller. In contrast to the proposed controller with PDS, the response of the controller with PD left some vibrations. After 10 seconds by conducting the controller with PD, the vibration amplitude is larger than 0.2m from Fig. 4(a), and the vibration velocity is faster 0.8m/s from Fig. 4(d). The root mean squared error value of $w(L,t)$ in the response of the controller with PDS was $E_{w(L,t)} = \|w(L,t) - w_\epsilon(L)\| = 0.1073$, while this value in the controller with PD flexible arm control was $E_{w(L,t)} = \|w(L,t) - w_\epsilon(L)\| = 0.1736$. These results indicate that the proposed controller with PDS flexible arm control had higher performance than the controller with PD flexible arm control.

Fig. 6 shows the evaluation of nonlinear coupling item d_τ that is considered a disturbance, where the dashed line shows the real value while the solid line is the evaluation. It shows

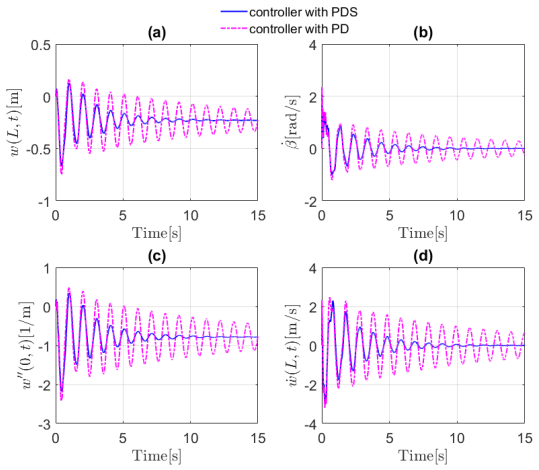

FIGURE 4. Comparison of deformation of end effector.

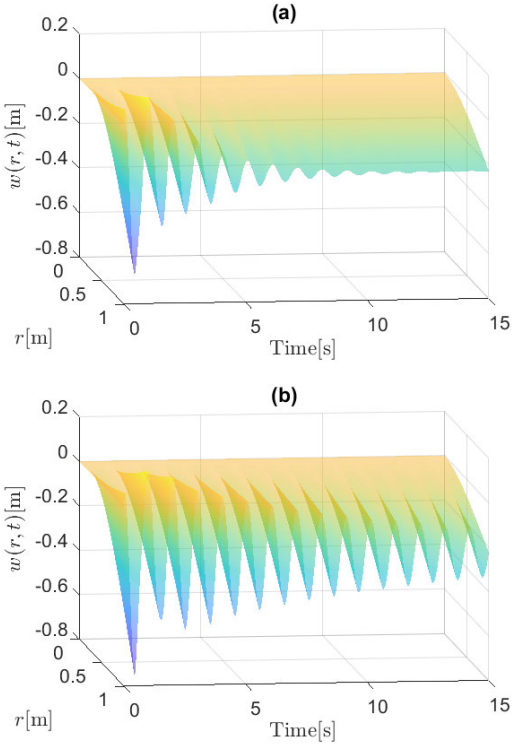

FIGURE 5. Deformation of the flexible arm. (a) is under the controller with PDS while (b) is with PD.

that the disturbance observer worked well in both PDS control and PD control.

C. SIMULATION 2

In order to investigate the response of the proposed controller under the conditions closed to the real world, we conducted numerical simulations with input disturbances and measurement noises to the quadrotor UAV as follows:

(1) Adding $0.5\sin(t)$N and $0.02\sin(t)$Nm into f_B and τ_B respectively.

(2) Adding random noise to state variables x and z with maximum amplitude 0.005m.

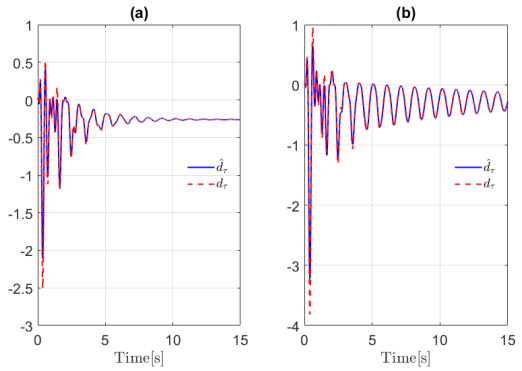

FIGURE 6. Evaluations by disturbance observer. (a) is under the controller with PDS while (b) is with PD.

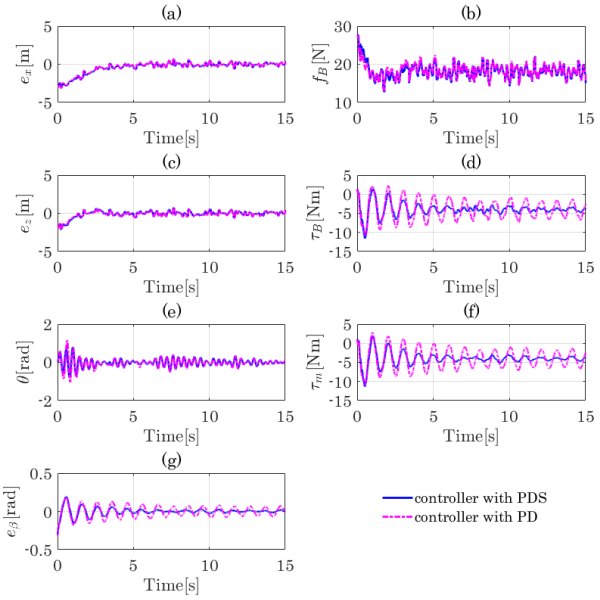

FIGURE 7. Responses of states and needed inputs under input disturbances and measurement noises.

The feedback gains, initial state, and desired positions are same with the simulations in Section V-B.

Simulation results are shown in Fig. 7-Fig. 10. In Fig. 7 and Fig. 8,same with simulation 1, the solid lines show the responses of the controller with PDS flexible arm control, while the stippled lines show the response of the controller with PD flexible arm control.

From the states' responses in Fig. 7(a)(c)(e)(g), Fig. 8, and Fig. 9, we can find that there are obvious oscillation phenomena comparing with the case without disturbance and noise in Section V.B. In Fig. 7, (b)(d) show the required force and torque of the quadrotor UAV, and (f) shows the required torque of the arm motor as the control input. These values are reasonable for real actuators. Fig. 10 shows that the disturbance observer in presence of input disturbances and measurement noises also worked well in both PDS control and PD control, where the dashed line shows the real value while the solid line is the evaluation.

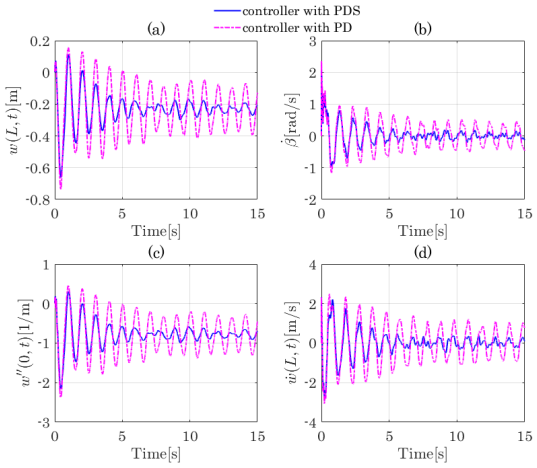

FIGURE 8. Deformation of end effector under input disturbances and measurement noises.

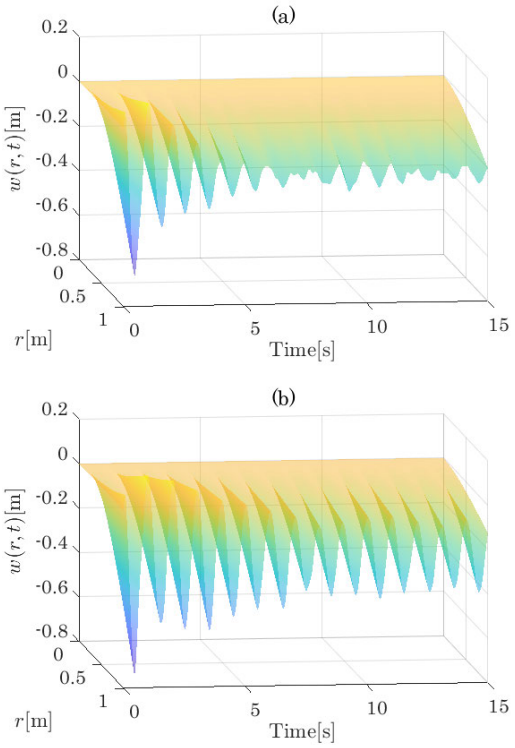

FIGURE 9. Deformation of the flexible arm under input disturbances and measurement noises.

Under the input disturbances and measurement noises, the proposed controller with PDS flexible arm control had higher performance than the controller with PD flexible arm control, which is indicated by the angle error e_β and transverse displacement $w(L,t)$. The root mean squared error value of e_β in the response of the controller with PDS flexible arm control was $E_{e_\beta} = \|e_\beta\| = 0.0519$, while this value in the controller with PD flexible arm control was $E_{e_\beta} = \|e_\beta\| = 0.0778$, where $\|\cdot\| = \sqrt{\frac{1}{N}\Sigma_1^N(\cdot)^2}$ and N is the total number of samples. The root mean squared error value

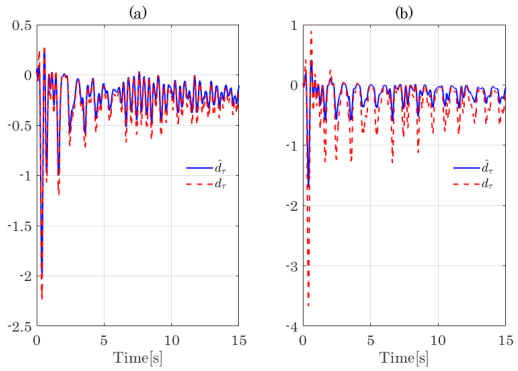

FIGURE 10. Evaluations by disturbance observer under input disturbances and measurement noises. (a) is under the controller with PDS while (b) is with PD.

of $w(L,t)$ in the response of the controller with PDS was $E_{w(L,t)} = \|w(L,t) - w_\epsilon(L)\| = 0.1074$, while this value in the controller with PD flexible arm control was $E_{w(L,t)} = \|w(L,t) - w_\epsilon(L)\| = 0.1738$.

VI. CONCLUSION

In this paper, the control problem for a quadrotor UAV equipped with a one-link Euler-Bernoulli arm was considered based on a hybrid PDE-ODE model. First, the dynamic model was derived using Hamilton's principle. Then, a simple controller with a disturbance observer was proposed based on the Lyapunov method. The proposed controller achieved motion control of the aerial manipulation system and suppressed the vibration of the flexible arm at the same time. Specifically, the asymptotic stability of the closed-loop system was proved by LaSalle's invariance principle applied to infinite-dimensional systems in the neighborhood of the desired state. Finally, through numerical simulations, we confirmed that the proposed controller works well during both hovering and motion.

In this paper, a motion in the vertical plane was considered. In future research, it would be desirable to investigate the control problem in a 3D environment and to conduct an experimental implementation.

APPENDIX A
CALCULATION OF $\dot{V}_1$

According to Eqns. (5) and (6), we can obtain time derivative equations as follows:

$$\dot{K}_{Bt} = m_b\dot{x}\ddot{x} + m_b\dot{z}\ddot{z}, \quad \dot{K}_M = J_m\dot{\beta}\ddot{\beta}, \tag{69}$$

$$\begin{aligned}\dot{K}_A &= \rho\int_0^L (\dot{p}_{rx}\ddot{p}_{rx} + \dot{p}_{rz}\ddot{p}_{rz})dr \\ &= \dot{\beta}\left(\int_0^L -\rho\ddot{p}_{rx}(rS_\beta - C_\beta w)dr \right. \\ &\quad \left. - \int_0^L \rho\ddot{p}_{rz}(rC_\beta + S_\beta w)dr\right) \\ &\quad + \int_0^L \rho\left(\dot{w}(S_\beta\ddot{p}_{rx} + C_\beta\ddot{p}_{rz}) + \dot{x}\ddot{p}_{rx} + \dot{z}\ddot{p}_{rz}\right)dr, \end{aligned}\tag{70}$$

$$\begin{aligned}\dot{K}_E &= m_e(\dot{p}_{ex}\ddot{p}_{ex} + \dot{p}_{ez}\ddot{p}_{ez}) \\ &= \dot{\beta}\left(-m_e\ddot{p}_{ex}\left(LS_\beta - C_\beta w_e\right) - m_e\ddot{p}_{ez}\left(LC_\beta + S_\beta w_e\right)\right) \\ &\quad + m_e\dot{w}_e\left(S_\beta\ddot{p}_{ex} + C_\beta\ddot{p}_{ez}\right) + m_e(\dot{x}\ddot{p}_{ex} + \dot{z}\ddot{p}_{ez}), \end{aligned}\tag{71}$$

$$\begin{aligned}\dot{U}_w &= \int_0^L \rho g\left(\dot{w}C_\beta - w\dot{\beta}S_\beta\right)dr + m_e g\left(\dot{w}_e C_\beta - w_e\dot{\beta}S_\beta\right) \\ &\quad + \int_0^L \mathrm{EI}w''(\dot{w}'')dr. \end{aligned}\tag{72}$$

Using integration by parts and the boundary conditions $w(0,t) = 0$, $w'(0,t) = 0$, and $w_e'' = 0$ in Eq. (9), we know that

$$\begin{aligned}&\int_0^L EIw''(\dot{w}'')dr \\ &= EIw''(\dot{w}')\,|_0^L - \int_0^L EIw'''(\dot{w}')dr \\ &= EIw''(\dot{w}')\,|_0^L - EIw'''\dot{w}\,|_0^L + \int_0^L EIw''''\dot{w}dr \\ &= -EIw_e'''\dot{w}_e + \int_0^L EIw''''\dot{w}dr. \end{aligned}\tag{73}$$

By combining above Eqns. (69)-(73), we have

$$\begin{aligned}\dot{V}_1 &= \dot{K}_{Bt} + \dot{K}_M + \dot{K}_A + \dot{K}_E + \dot{U}_w \\ &= \left(m_b\ddot{x} + \int_0^L \rho\ddot{p}_{rx}dr + m_e\ddot{p}_{ex}\right)\dot{x} \\ &\quad + \left(m_b\ddot{z} + \int_0^L \rho\ddot{p}_{rz}dr + m_e\ddot{p}_{ez}\right)\dot{z} \\ &\quad + \left\{-\int_0^L \rho\ddot{p}_{rx}\left(rS_\beta - wC_\beta\right)dr \right. \\ &\qquad - \int_0^L \rho\ddot{p}_{rz}\left(rC_\beta + wS_\beta\right)dr \\ &\qquad -m_e\ddot{p}_{ex}\left(LS_\beta - w_eC_\beta\right) - m_e\ddot{p}_{ez}\left(LC_\beta + w_eS_\beta\right) \\ &\qquad \left. - \int_0^L \rho gS_\beta wdr - m_e g w_e S_\beta + J_m\ddot{\beta}\right\}\dot{\beta} \\ &\quad + \left(m_e\ddot{p}_{ex}S_\beta + m_e\ddot{p}_{ez}C_\beta + m_e gC_\beta - EIw_e'''\right)\dot{w}_e \\ &\quad + \int_0^L \left(\rho\ddot{p}_{rx}S_\beta + \rho\ddot{p}_{rz}C_\beta + \rho gC_\beta + EIw''''\right)\dot{w}dr, \end{aligned}\tag{74}$$

and from the derivation procedure of Eq. (8) to Eq. (9), we can know

$$\begin{cases} m_b\ddot{x} + \int_0^L \rho\ddot{p}_{rx}dr + m_e\ddot{p}_{ex} = \theta f_B, \\ m_b\ddot{z} + \int_0^L \rho\ddot{p}_{rz}dr + m_e\ddot{p}_{ez} = f_B - m_0 g, \\ -\int_0^L \rho\ddot{p}_{rx}\left(rS_\beta - wC_\beta\right)dr - \int_0^L \rho\ddot{p}_{rz}\left(rC_\beta + wS_\beta\right)dr \\ \quad -m_e\ddot{p}_{ex}\left(LS_\beta - w_eC_\beta\right) - m_e\ddot{p}_{ez}\left(LC_\beta + w_eS_\beta\right) \\ \quad - \int_0^L \rho gS_\beta wdr - m_e g w_e S_\beta + J_m\ddot{\beta} = \tau_m + G, \\ m_e\ddot{p}_{ex}S_\beta + m_e\ddot{p}_{ez}C_\beta + m_e gC_\beta - EIw_e''' = 0, \\ \rho\ddot{p}_{rx}S_\beta + \rho\ddot{p}_{rz}C_\beta + \rho gC_\beta + EIw'''' = 0, \end{cases}\tag{75}$$

where $G = \int_0^L \rho g r C_\beta dr + m_e g L C_\beta = (\frac{1}{2}m_a + m_e) g L C_\beta$. Substituting (75) into (74), then we obtain Eq. (28) as follow:

$$\dot{V}_1 = \dot{x}\theta f_B + \dot{z}(f_B - m_0 g) + \dot{\beta}\,(\tau_m + G)\,.$$

APPENDIX B
PROOF OF LEMMA 1

Since H together with the standard inner product would be a Hilbert space, we would like to show that the norm induced by the inner product (37) is equivalent to that of the standard one. In other words, we show that the norm,

$$\begin{aligned}\| u \|_1^2 = {} & \frac{1}{2}m_0(v_1^2 + v_2^2) + \frac{1+k_7}{2}J_m v_3^2 \\ & + \frac{1}{2}\int_0^L \rho v_w^2 dr + \frac{1}{2}\int_0^L EI(u_w'')^2 dr + \frac{1}{2}m_e v_e^2 \\ & + \frac{k_1}{2}u_1^2 + \frac{k_5}{2}u_2^2 + \frac{k_8}{2}u_3^2 + \frac{k_3k_4+1}{2}u_4^2 + \frac{1}{2}v_4^2, \quad (76)\end{aligned}$$

is equivalent to the norm,

$$\begin{aligned}\| u \|_2^2 = {} & \int_0^L \left(u_w^2 + (u_w')^2 + (u_w'')^2\right) dr + \int_0^L v_w^2 dr + v_e^2 \\ & + u_1^2 + u_2^2 + u_3^2 + u_4^2 + v_1^2 + v_2^2 + v_3^2 + v_4^2. \quad (77)\end{aligned}$$

Next, we show that there exist positive constants α_1 and α_2 satisfying with

$$\alpha_1 \| u \|_2^2 \le \| u \|_1^2, \quad (78)$$

$$\| u \|_1^2 \le \alpha_2 \| u \|_2^2\,. \quad (79)$$

Here, we note that

$$u_w = \int_0^r u_w' dr + u_w(0),$$

by using the inequality

$$|\, a+b \,|^2 \le (|\, a \,| + |\, b \,|)^2 \le 2(|\, a \,|^2 + |\, b \,|^2), \quad (80)$$

and boundary condition $u_w(0) = S_{\beta_d}u_1 + C_{\beta_d}u_2$, thus we have

$$\begin{aligned}u_w^2 &\le 2\left(\int_0^L u_w' dr\right)^2 + 2u_w^2(0) \\ &\le 2\left(\int_0^L u_w' dr\right)^2 + 4u_1^2 + 4u_2^2. \quad (81)\end{aligned}$$

And from Cauchy-Schwarz inequality

$$\left\{\int_a^b h(x)\hat{h}(x)dx\right\}^2 \le \int_a^b h^2(x)dx \int_a^b \hat{h}^2(x)dx, \quad (82)$$

then we know that Eq. (81) satisfy with

$$u_w^2 \le 2L\int_0^L (u_w')^2 dr + 4u_1^2 + 4u_2^2.$$

Integrating above relation derives

$$\int_0^L u_w^2 dr \le 2L^2 \int_0^L (u_w')^2 dr + 4Lu_1^2 + 4Lu_2^2. \quad (83)$$

Similarly, for $u_w' = \int_0^r u_w'' dr + u_w'(0)$, we have

$$\int_0^L (u_w')^2 dr \le 2L^2 \int_0^L (u_w'')^2 dr + 2Lu_3^2. \quad (84)$$

Therefore,

$$\begin{aligned}\| u \|_2^2 = {} & \int_0^L u_w^2 dr + \int_0^L (u_w')^2 dr + \int_0^L (u_w'')^2 dr + \int_0^L v_w^2 dr \\ & + v_e^2 + u_1^2 + u_2^2 + u_3^2 + u_4^2 + v_1^2 + v_2^2 + v_3^2 + v_4^2 \\ \le {} & (1+2L^2)\int_0^L (u_w')^2 dr + \int_0^L (u_w'')^2 dr + \int_0^L v_w^2 dr \\ & + v_e^2 + (4L+1)u_1^2 + (4L+1)u_2^2 + u_3^2 + u_4^2 \\ & + v_1^2 + v_2^2 + v_3^2 + v_4^2 \\ \le {} & (1+2L^2+4L^4)\int_0^L (u_w'')^2 dr + \int_0^L v_w^2 dr \\ & + v_e^2 + (4L+1)u_1^2 + (4L+1)u_2^2 + (2L+1)u_3^2 \\ & + u_4^2 + v_1^2 + v_2^2 + v_3^2 + v_4^2,\end{aligned}$$

where we used Eq. (83) and (84). Defining the set

$$\Upsilon = \{EI, \rho, m_e, k_1, k_5, k_8, (k_3k_4+1), m_0, (1+k_7)J_m, 1\},$$

and letting

$$\begin{aligned}\alpha_1 &\le \frac{\min \Upsilon}{2(1+2L^2+4L^4)}, \\ \alpha_2 &\ge \frac{\max \Upsilon}{2(1+2L^2+4L^4)},\end{aligned}$$

then Eqns. (78) and (79) hold. Thus, the norm $\| u \|_1^2$ is equivalent to the norm $\| u \|_2^2$ from Eqns. (78) and (79).

APPENDIX C
DERIVATION DETAILS OF INNER PRODUCT CALCULATION

For any given $y = [u_1, v_1, u_2, v_2, u_3, v_3, u_4, v_4, v_e, u_w, v_w]^T \in D(A)$, according to Eqns. (37) and (40), we have

$$\begin{aligned}&\langle Ay, y\rangle_H \\ &= \left\langle \begin{bmatrix} v_1 \\ -\frac{k_1}{m_0}u_1 - \frac{k_2}{m_0}v_1 \\ v_2 \\ -\frac{k_5}{m_0}u_2 - \frac{k_6}{m_0}v_2 \\ v_3 \\ \frac{1}{J_m(1+k_7)}\left(-k_8u_3 - k_9 v_3 - EIu_w''(0)\right) \\ v_4 \\ -(k_3k_4+1)u_4 - (k_3+k_4)v_4 \\ \frac{EI}{m_e}u_w'''(L) \\ v_w \\ -\frac{EI}{\rho}u_w'''' \end{bmatrix}, \begin{bmatrix} u_1 \\ v_1 \\ u_2 \\ v_2 \\ u_3 \\ v_3 \\ u_4 \\ v_4 \\ v_e \\ u_w \\ v_w \end{bmatrix} \right\rangle_H \\ &= \frac{1}{2}m_0\left(\left(-\frac{k_1}{m_0}u_1 - \frac{k_2}{m_0}v_1\right)v_1 + \left(-\frac{k_5}{m_0}u_2 - \frac{k_6}{m_0}v_2\right)v_2\right) \\ &\quad + \frac{1+k_7}{2}J_m\frac{1}{J_m(1+k_7)}\left(-k_8u_3 - k_9v_3 - EIu_w''(0)\right)v_3\end{aligned}$$

$$+\frac{1}{2}\int_0^L \rho(-\frac{EI}{\rho}u_w'''')v_w dr+\frac{1}{2}\int_0^L EIv_w''u_w'' dr$$
$$+\frac{1}{2}m_e\frac{EI}{m_e}u_w'''(L)v_e+\frac{k_1}{2}v_1u_1+\frac{k_5}{2}v_2u_2+\frac{k_8}{2}v_3u_3$$
$$+\frac{k_3k_4+1}{2}v_4u_4+\frac{1}{2}\left(-(k_3k_4+1)u_4-(k_3+k_4)v_4\right)v_4$$
$$=-\frac{k_2}{2}v_1^2-\frac{k_6}{2}v_2^2-\frac{k_9}{2}v_3^2-\frac{1}{2}EI\left(u_w''(0)v_3+\int_0^L u_w''''v_w dr\right.$$
$$\left.-\int_0^L v_w''u_w'' dr-u_w'''(L)v_e\right)-\frac{k_3}{2}u_4^2-\frac{k_3+k_4}{2}v_4^2. \quad (85)$$

Using integration by parts and the boundary conditions $v_w(L)=v_e$, $v_w(0)=0$, $u_w''(L)=0$, $v_w'(0)=-v_3$ in Eq. (41), then we know that

$$\begin{aligned}\int_0^L u_w''''v_w dr &= u_w'''v_w\mid_0^L-\int_0^L u_w'''v_w' dr\\ &= u_w'''(L)v_w(L)-u_w'''(0)v_w(0)-\int_0^L u_w'''v_w' dr\\ &= u_w'''(L)v_e-u_w''v_w'\mid_0^L+\int_0^L u_w''v_w'' dr\\ &= u_w'''(L)v_e-u_w''(0)v_3+\int_0^L u_w''v_w'' dr. \quad (86)\end{aligned}$$

Therefore, Eq. (85) can be rewritten as

$$\langle Ay,y\rangle_H=-\frac{k_2}{2}v_1^2-\frac{k_6}{2}v_2^2-\frac{k_9}{2}v_3^2-\frac{k_3}{2}u_4^2-\frac{k_3+k_4}{2}v_4^2,$$

which is shown in Eq. (43).

APPENDIX D
PROOF OF EXISTENCE OF K

The main concern is whether $\| u_w \|^2=\int_0^L u_w^2 dr$ is upper bounded or not. According to the Cauchy-Schwarz inequality Eq. (82), we have

$$\begin{aligned}u_w &= c_{w0}+c_{w1}r+\frac{c_{w2}}{2}r^2+\frac{c_{w3}}{6}r^3\\ &\quad+\frac{\rho}{EI}\int_0^r\int_0^{r_1}\int_0^{r_2}\int_0^{r_3}h_w(r_4)dr_4dr_3dr_2dr_1\\ &= c_{w0}+c_{w1}r+\frac{c_{w2}}{2}r^2+\frac{c_{w3}}{6}r^3\\ &\quad+\frac{\rho}{6EI}\int_0^r(r-r_4)^3h_w(r_4)dr_4,\\ &\le c_{w0}+c_{w1}r+\frac{c_{w2}}{2}r^2+\frac{c_{w3}}{6}r^3\\ &\quad+\frac{\rho}{6EI}\left\{\int_0^r(r-r_4)^6dr_4\int_0^r h_w^2(r_4)dr_4\right\}^{\frac{1}{2}}. \quad (87)\end{aligned}$$

Besides, from boundary conditions, we can get

$$\begin{aligned}c_{w0} &= u_w(0)=S_{\beta_d}u_1+C_{\beta_d}u_2,\\ c_{w1} &= u_w'(0)=-u_3,\\ c_{w2} &= u_w''(0)=-c_{w3}L-\frac{\rho}{EI}\int_0^L(r-r_4)h_w(r_4)dr_4,\\ c_{w3} &= -\frac{\rho}{EI}\int_0^L h_w(r)dr-\frac{m_e}{EI}h_e.\end{aligned}$$

By using the inequality Eq. (80), then we have

$$\begin{aligned}c_{w0}^2 &\le K_0\left\{h_1^2+l_1^2+h_2^2+l_2^2\right\},\\ c_{w1}^2 &\le K_1\left\{h_3^2+l_3^2+\|h_w\|^2+h_e^2\right\},\\ c_{w2}^2 &\le K_2\left\{\|h_w\|^2+h_e^2\right\},\\ c_{w3}^2 &\le K_3\left\{\|h_w\|^2+h_e^2\right\}. \quad (88)\end{aligned}$$

And thus, we can obtain

$$\int_0^L u_w^2 dr\le K_4\left\{\|h_w\|^2+h_e^2+h_1^2+h_2^2+h_3^2+l_1^2+l_2^2+l_3^2\right\}. \quad (89)$$

Therefore, we now know that $\| u_w \|^2=\int_0^L u_w^2 dr$ is upper bounded. Please note that $\| * \|^2=\int_0^L *^2 dr$ in this work, and $K_j>0(j=0,1,\cdots,4)$.

By applying this procedure with other variables, then we can prove Eq.(45) is available:

$$\| \phi \|_H=\| A^{-1}\psi \|_H\le K\| \psi \|_H .$$

REFERENCES

[1] L. Díaz-Vilariño, H. González-Jorge, J. Martínez-Sánchez, M. Bueno, and P. Arias, "Determining the limits of unmanned aerial photogrammetry for the evaluation of road runoff," *Measurement*, vol. 85, pp. 132–141, May 2016.
[2] Z. Cui, J. Yang, and S. Jiang, "An infrared small target detection algorithm based on high-speed local contrast method," *Infr. Phys. Technol.*, vol. 76, pp. 474–481. May 2016.
[3] S. Gallardo-Saavedra, L. Hernández-Callejo, and O. Duque-Perez, "Technological review of the instrumentation used in aerial thermographic inspection of photovoltaic plants," *Renew. Sustain. Energy Rev.*, vol. 93, pp. 566–579, Oct. 2018.
[4] F. Ruggiero, V. Lippiello, and A. Ollero, "Aerial manipulation: A literature review," *IEEE Robot. Autom. Lett.*, vol. 3, no. 3, pp. 1957–1964, Jul. 2018.
[5] X. Ding, P. Guo, K. Xu, and Y. Yu, "A review of aerial manipulation of small-scale rotorcraft unmanned robotic systems," *Chin. J. Aeronaut.*, vol. 32, no. 1, pp. 200–214, Jan. 2019.
[6] J. Kim, S. Kim, C. Ju, and H. I. Son, "Unmanned aerial vehicles in agriculture: A review of perspective of platform, control, and applications," *IEEE Access*, vol. 7, pp. 105100–105115, 2019.
[7] A. Suarez, V. M. Vega, M. Fernandez, G. Heredia, and A. Ollero, "Benchmarks for aerial manipulation," *IEEE Robot. Autom. Lett.*, vol. 5, no. 2, pp. 2650–2657, Apr. 2020.
[8] D. Mellinger, Q. Lindsey, M. Shomin, and V. Kumar, "Design, modeling, estimation and control for aerial grasping and manipulation," in *Proc. IEEE/RSJ Int. Conf. Intell. Robots Syst.*, San Francisco, CA, USA, Sep. 2011, pp. 2668–2673.
[9] J. Thomas, J. Polin, K. Sreenath, and V. Kumar, "Avian-inspired grasping for quadrotor micro UAVs," in *Proc. 37th Mech. Robot. Conf.*, Portland, OR, USA, Aug. 2013, pp. 1–9.
[10] A. Khalifa and M. Fanni, "Experimental implementation of a new non-redundant 6-DOF quadrotor manipulation system," *ISA Trans.*, vol. 104, pp. 345–355, Sep. 2020.
[11] M. Jafarinasab, S. Sirouspour, and E. Dyer, "Model-based motion control of a robotic manipulator with a flying multirotor base," *IEEE/ASME Trans. Mechatronics*, vol. 24, no. 5, pp. 2328–2340, Oct. 2019.
[12] H. Zhong, Z. Miao, Y. Wang, J. Mao, L. Li, H. Zhang, Y. Chen, and R. Fierro, "A practical visual servo control for aerial manipulation using a spherical projection model," *IEEE Trans. Ind. Electron.*, vol. 67, no. 12, pp. 10564–10574, Dec. 2020.
[13] M. Orsag, C. Korpela, S. Bogdan, and P. Oh, "Dexterous aerial robots—Mobile manipulation using unmanned aerial systems," *IEEE Trans. Robot.*, vol. 33, no. 6, pp. 1453–1466, Dec. 2017.
[14] A. Suarez, P. R. Soria, G. Heredia, B. C. Arrue, and A. Ollero, "Anthropomorphic, compliant and lightweight dual arm system for aerial manipulation," in *Proc. IEEE/RSJ Int. Conf. Intell. Robots Syst. (IROS)*, Vancouver, BC, Canada, Sep. 2017, pp. 992–997.

[15] T. Ikeda, S. Yasui, M. Fujihara, K. Ohara, S. Ashizawa, A. Ichikawa, A. Okino, T. Oomichi, and T. Fukuda, "Wall contact by octo-rotor UAV with one DoF manipulator for bridge inspection," in *Proc. IEEE/RSJ Int. Conf. Intell. Robots Syst. (IROS)*, Vancouver, BC, Canada, Sep. 2017, pp. 5122–5127.
[16] B. Yüksel, C. Secchi, H. H. Bülthoff, and A. Franchi, "Aerial physical interaction via IDA-PBC," *Int. J. Robot. Res.*, vol. 38, no. 4, pp. 403–421, Apr. 2019.
[17] T. Wang, K. Umemoto, T. Endo, and F. Matsuno, "Dynamic hybrid position/force control for the quadrotor with a multi-degree-of-freedom manipulator," *Artif. Life Robot.*, vol. 24, no. 3, pp. 378–389, Feb. 2019.
[18] O. Satoshi, K. Ohara, T. Ikeda, A. Ichikawa, S. Asizawa, T. Oomichi, and T. Fukuda, "Light weight manipulator on UAV system for infrastructure inspection," in *Proc. Int. Symp. Micro-NanoMechatron. Human Sci.*, Nagoya, Japan, Dec. 2017, pp. 1–3.
[19] L. Fang, H. Chen, Y. Lou, Y. Li, and Y. Liu, "Visual grasping for a lightweight aerial manipulator based on NSGA-II and kinematic compensation," in *Proc. IEEE Int. Conf. Robot. Autom. (ICRA)*, Brisbane, QLD, Australia, May 2018, pp. 3488–3493.
[20] M. Orsag, C. Korpela, and P. Oh, "Modeling and control of MM-UAV: Mobile manipulating unmanned aerial vehicle," *J. Intell., Robotic Syst.*, vol. 69, nos. 1–4, pp. 227–240, 2013.
[21] A. Suarez, G. Heredia, and A. Ollero, "Lightweight compliant arm with compliant finger for aerial manipulation and inspection," in *Proc. IEEE/RSJ Int. Conf. Intell. Robots Syst. (IROS)*, Daejeon, South Korea, Oct. 2016, pp. 4449–4454.
[22] X. Sheng, Z. Ma, N. Zhang, and W. Dong, "Aerial contact manipulation with soft end-effector compliance and inverse kinematic compensation," *J. Mech. Robot.*, vol. 13, no. 1, pp. 11–23, Feb. 2021.
[23] A. Suarez, A. E. Jimenez-Cano, V. M. Vega, G. Heredia, A. Rodriguez-Castaño, and A. Ollero, "Design of a lightweight dual arm system for aerial manipulation," *Mechatronics*, vol. 50, pp. 30–44, Apr. 2018.
[24] A. Suarez, F. Real, V. M. Vega, G. Heredia, A. Rodriguez-Castano, and A. Ollero, "Compliant bimanual aerial manipulation: Standard and long reach configurations," *IEEE Access*, vol. 8, pp. 88844–88865, 2020.
[25] A. Suarez, P. J. Sanchez-Cuevas, G. Heredia, and A. Ollero, "Aerial physical interaction in grabbing conditions with lightweight and compliant dual arms," *Appl. Sci.*, vol. 10, no. 24, pp. 1–17, Dec. 2020.
[26] A. Suarez, P. Sanchez-Cuevas, M. Fernandez, M. Perez, G. Heredia, and A. Ollero, "Lightweight and compliant long reach aerial manipulator for inspection operations," in *Proc. IEEE/RSJ Int. Conf. Intell. Robots Syst. (IROS)*, Madrid, Spain, Oct. 2018, pp. 6746–6752.
[27] M. J. Balas, "Feedback control of flexible systems," *IEEE Trans. Autom. Control*, vol. AC-23, no. 4, pp. 673–679, Aug. 1978.
[28] Q. Wei and L. Wang, "Exponential stabilisation of Euler–Bernoulli beam with uncertain disturbance," *Int. J. Control*, vol. 94, pp. 1–8, Sep. 2019.
[29] X. Xing and J. Liu, "PDE model-based state-feedback control of constrained moving vehicle-mounted flexible manipulator with prescribed performance," *J. Sound Vib.*, vol. 441, pp. 126–151, Feb. 2019.
[30] T. Endo, F. Matsuno, and H. Kawasaki, "Simple boundary cooperative control of two one-link flexible arms for grasping," *IEEE Trans. Autom. Control*, vol. 54, no. 10, pp. 2470–2476, Oct. 2009.
[31] T. Endo, K. Umemoto, and F. Matsuno, "Exponential stability of dual flexible arms for grasping and orientation control," *IET Control Theory Appl.*, vol. 13, no. 16, pp. 2546–2555, Nov. 2019.
[32] Z.-D. Mei, "Dynamic stabilisation for an Euler–Bernoulli beam equation with boundary control and matched nonlinear disturbance," *Int. J. Control*, pp. 1–15, Aug. 2020.
[33] T. Endo, F. Matsuno, and H. Kawasaki, "Force control and exponential stabilisation of one-link flexible arm," *Int. J. Control*, vol. 87, no. 9, pp. 1794–1807, Mar. 2014.
[34] T. Endo, F. Matsuno, and Y. Jia, "Boundary cooperative control by flexible Timoshenko arms," *Automatica*, vol. 81, pp. 377–389, Jul. 2017.
[35] H. K. Rad, H. Salarieh, A. Alasty, and R. Vatankhah, "Boundary control of flexible satellite vibration in planar motion," *J. Sound Vib.*, vol. 432, pp. 549–568, Oct. 2018.
[36] F. Han and Y. Jia, "Boundary control and exponential stability of a flexible timoshenko beam manipulator with measurement delays," *IET Control Theory Appl.*, vol. 14, no. 3, pp. 499–510, Feb. 2020.
[37] K. Umemoto, T. Endo, F. Matsuno, and T. Egami, "Stability analysis of a control system with nonlinear input uncertainty based on disturbance observer," *Int. J. Robust Nonlinear Control*, vol. 30, no. 11, pp. 4433–4448, Apr. 2020.
[38] Z. Liu and S. Zheng, *Semigroups Associated With Dissipative Systems*. Boca Raton, FL, USA: CRC Press, 1999.
[39] A. Pazy, *Semigroups of Linear Operators and Applications to Partial Differential Equations*. New York, NY, USA: Springer-Verlag, 1983.
[40] Z. Luo, B. Guo, and O. Morgül, *Stability and Stabilization of Infinite Dimensional Systems With Applications*. London, U.K.: Springer-Verlag, 1999.
[41] T. Kato, *Perturbation Theory for Linear Operators*. Berlin, Germany: Springer-Verlag, 1995.
[42] Y. Sakawa, F. Matsuno, and S. Fukushima, "Modeling and feedback control of a flexible arm," *J. Robot. Syst.*, vol. 2, no. 4, pp. 453–472, 1985.

TIEHUA WANG received the B.E. degree in mechanical and electrical engineering from the Beijing University of Chemical Technology, China, in 2010, and the M.E. degree in mechanical engineering and automation from Beihang University, China, in 2013. He is currently pursuing the Ph.D. degree in mechanical engineering and science with Kyoto University, Japan. His research interests include nonlinear and robust control, unmanned aerial vehicles, aerial manipulation systems, and infinite-dimensional systems.

KAZUKI UMEMOTO (Member, IEEE) received the B.E. and M.E. degrees from Okayama University, in 2008 and 2010, respectively, and the Ph.D. degree from Kyoto University, in 2014. He joined the Department of Mechanical Engineering, Kanagawa University, Kanagawa, Japan. Since 2017, he has been with the Department of Mechanical Engineering, Nagaoka University of Technology, Niigata, Japan. His main research interests include nonlinear control and robust control.

TAKAHIRO ENDO (Member, IEEE) received the Ph.D. (Dr.Eng.) degree from the Tokyo Institute of Technology, Japan, in 2006. He was an Assistant Professor with Gifu University, Gifu, Japan. Since April 2015, he has been with the Department of Mechanical Engineering and Science, Kyoto University, Kyoto, Japan, where he is currently an Associate Professor. His research interests include haptics, robotics, and the control of infinite-dimensional systems.

FUMITOSHI MATSUNO (Senior Member, IEEE) received the Ph.D. (Dr.Eng.) degree from Osaka University, Toyonaka, Japan, in 1986.

In 1986, he joined the Department of Control Engineering, Osaka University. Since 2009, he has been a Professor with the Department of Mechanical Engineering and Science, Kyoto University, Kyoto, Japan. He is also the Vice President of the NPO International Rescue System Institute, Kobe, Japan, and served as the President for the Institute of Systems, Control and Information Engineers and the Vice President for the Robotics Society of Japan (RSJ). His current research interests include robotics, swarm intelligence, the control of distributed parameter systems and nonlinear systems, and rescue support systems in disaster. He is a Fellow Member of the SICE, the JSME, and the RSJ. He received many awards, including the Outstanding Paper Award, in 2001, 2006, and 2017, the Takeda Memorial Prize, in 2001, and the Tomoda Memorial Prize from the Society of Instrument and Control Engineers (SICE), the Prize for Academic Achievement from Japan Society of Mechanical Engineers (JSME), in 2009, the Best Paper Award from the Information Processing Society of Japan, in 2013, and the Best Paper Award from the RSJ, in 2018. He is a General Chair of DARS-SWARM2021 and a Co-General Chair of ASCC2022. He served as a General Chair for the IEEE SSRR2011 and the IEEE/SICE SII2011, SWARM2015, and SWARM2017.